

1800 Copy
(Version reviewed)

CONF-950739-1
SAND094-3230C

FAILURE ANALYSIS OF A FIBERGLASS-REINFORCED PLASTIC PRESSURE VESSEL

S. J. Glass, E. K. Beauchamp, M. Carr, T. R. Guess, S. L. Monroe, R. J. Moore, A. Slavin, and N. R. Sorenson, Sandia National Laboratories, Albuquerque, NM 87185.

ABSTRACT

A fiberglass-reinforced plastic (FRP) pressure vessel containing sulfuric acid failed catastrophically in service. Preliminary investigations ruled out failure due to sabotage and chemical or mechanical overpressure. Subsequent examination of the fiber fracture surfaces and measurements of mirror radii indicated that fiber failure had occurred at stresses significantly below the fibers' expected strength. Further examination by scanning electron microscopy and energy dispersive spectroscopy indicated that the glass fibers had been exposed to sulfuric acid, a reagent that corrodes this type of glass and degrades its strength. Finite element analysis indicated stresses in an exposed region of the vessel that exceeded the strengths of the FRP during normal vessel operation. Numerous cracks were detected in this region using a vicinal optical illumination technique. We concluded that vessel failure was caused by progressive degradation and rupture of fibers starting at the outer surface of the FRP and extending inwards and laterally, until a crack of critical size was produced.

BACKGROUND

A sulfuric acid vessel, pressurized at the normal operating pressure of 0.31 MPa (45 psi), burst during service. The vessel was one of two identical 200 liter, teflon-lined, fiberglass-reinforced plastic (FRP) vessels used as part of an acid distribution system. The FRP vessel contained several large cracks from which the burst teflon liner bulged as shown in Fig. 1A. The event also severely damaged the containment cabinet and showered the room with debris as shown in Fig. 1B. Although the room was unoccupied at the time of the failure, a thorough investigation of the event was performed in the interest of equipment reliability and personnel safety. Forensic

MASTER

S. Jill Glass

June 3, 1995

DISTRIBUTION OF THIS DOCUMENT IS UNLIMITED SEP 26 1995

DISCLAIMER

**Portions of this document may be illegible
in electronic image products. Images are
produced from the best available original
document.**

reconstruction of the event, fractographic analysis of the failed vessel, computer modeling of stresses in the vessel walls, and mechanical testing of sections of the failed vessel provided information about the cause of failure.

PRELIMINARY INVESTIGATION

During the preliminary investigation dozens of failure event scenarios were considered, all based on observations or recorded data. At each stage of the investigation, care was taken not to destroy or obscure evidence needed by a competing scenario. The various failure scenarios considered were grouped as follows:

- Sabotage
- Excessive internal pressure
 - Failure at elevated pressure due to chemical reaction.
(Sulfuric acid reacts violently with many compounds, including water)
 - Failure at elevated pressure due to mechanical over-pressurization
- Failure at normal operating conditions (pressure, temperature, environment)

There was no evidence to suggest that a person had the means or ability to cause this type of failure by sabotage. No evidence was found to uniquely support overpressure by chemical and/or mechanical means. Forensic evidence indicated that the pressure in the failed vessel was not unusually high when it failed. Trajectory analysis of debris, including a level sensor found fifteen feet away, indicated that the failure sequence was consistent with the FRP cracking, followed by the teflon bladder bulging out of the cracked FRP and bursting. A thorough analysis of the gas system also eliminated the possibility of mechanical over-pressurization. It was concluded that the failure occurred under normal operating conditions.

By design, the FRP vessels are expected to be able to withstand 200 psi pressure. That, of course, assumes that the vessel retains its integrity. Thus it was assumed that the vessel integrity must somehow have been compromised and subsequent investigation focused on the fracture surfaces, the mechanical properties of the FRP material, and the stress state in the vessel under normal operating pressure.

FRACTOGRAPHIC ANALYSES

Following an in situ examination of the ruptured FRP vessel, a three by twenty inch section (Fig. 1A, section in dashed lines) shown in Fig. 2, containing the primary fractures, was cut from the vessel for detailed examination. The axial location of these primary fractures is near the region on the vessel that was supported/constrained by the metal cradle and rubber gasket (Fig. 1A). The section of composite material containing the primary cracks is constructed from, nominally, seven layers (each ~0.05 cm

thick) of fiber-reinforced plastic with alternating + and -32° oriented fibers, termed cross plies. The cross plies are surrounded by a circumferential (circ) wrap (~0.23 cm thick) of fiber-reinforced plastic around the cylindrical portion of the vessel. The cross plies support the axial stresses in the vessel and the circ wraps support the hoop stresses.

Under normal conditions, overstressed FRP fails by a combination of epoxy matrix cracking and glass fiber pull-out. Where fibers are parallel or oriented at some small angle to the principal stress direction, the fracture surface will be very rough with extensive fiber pull-out. If the glass fibers are substantially weakened, little or no fiber pull-out occurs and the fracture surface will be planar because the failure mode is controlled by the matrix strength. Where fibers are oriented perpendicular to or almost perpendicular to the principal stress direction, as they are in the circ wrap, the fracture surface will also be planar with no protruding fibers.

Macroscopic examination of the primary fracture surface revealed two areas (Fig. 2, Areas A and B) of planar circumferential (or hoop) fracture, normal to the longitudinal axis of the vessel, extending almost completely through the circ wrap and cross plies as shown in the schematic in Fig. 3A. If the vessel is exposed to sufficiently high axial tensile stresses, this type of planar hoop crack is expected in the circ wrap (a result of interfacial failure between the fibers and the epoxy matrix), but not in the cross plies. Fracture in the cross plies should exhibit extensive fiber pull-out producing a fracture surface that is not planar (Fig. 3B). The planar fracture surface of the cross ply region was the first evidence that the vessel had been compromised in some way that weakened the fibers.

Areas A and B in Fig. 2 were examined using optical microscopy and scanning electron microscopy (SEM). SEM examination of a replica, taken from fracture A, provided evidence that the fracture propagated from the exterior toward the interior of the vessel. Individual fibers, in all of the cross plies, exhibited velocity hackle (Fig. 4), that indicated the direction of crack propagation was from the exterior to the interior. The fracture mirror radii also provided an estimate of the fiber failure stress.¹ Calculated failure stresses of these fibers ranged from 620 to 1207 MPa (90 to 175 ksi), substantially lower than the nominal 3100 MPa (450 ksi) strength for E-glass fibers used in the vessel construction.

Planar fracture regions were bounded by fracture regions exhibiting extensive fiber pull-out, which were likely created during the final moment of vessel rupture as the regions of planar fracture linked together. Fibers in these linking regions exhibited the mirror radii characteristic of failure stresses of 3100 MPa. These observations suggested that the vessel was

fabricated from E-glass fibers of the correct strength level, but that they had been degraded and weakened in some regions.

A portion of fracture B was examined using energy dispersive spectroscopy (EDS) to obtain chemical information on fiber composition and on the presence of corrosive agents. Because the fracture surface had been flooded with sulfuric acid during the vessel rupture and with aqueous solutions during clean-up, unequivocal chemical data could not be obtained from this area. Areas were sought for examination where cracks would not have been exposed to particulate debris, acid, or aqueous solutions. Chemical analyses were also performed on the fracture surfaces of flexure test specimens (described elsewhere in this paper) that were obtained from chemically uncompromised regions of the vessel. One specimen was selected for testing because it was located in the cradle region and contained a hoop crack in the circ wraps. This pre-existing crack did not extend completely through the specimen. The specimen was loaded in flexure such that the exterior surface containing the crack was placed in tension. This caused the pre-existing crack to propagate to completion through the innermost cross plies.

Figure 5 shows the fracture surfaces of a flexure specimen which did not contain a pre-existing crack (A) and the specimen described above that did (B). The direction of crack propagation is from the bottom of the figure proceeding towards the top. Figure 5A shows no planar fracture in the cross ply regions (Area 2). Figure 5B shows the two types of macroscopic fracture features in the cross plies, i.e., the pre-existing crack exhibits planar fracture (Fig. 5B, Area 1), whereas the fracture surface produced during testing exhibits the expected fiber pull-out (Fig. 5B, Area 2).

SEM examination of the fracture surface of the flexure bar with the pre-existing crack was performed. The pre-existing crack contained planar fracture both in the circ wrap and in some of the cross plies immediately adjacent to the circ wrap. The remainder of the cross plies, which failed during flexure testing, exhibited fiber pull-out (Fig. 6A) and the fibers in this region failed at high stresses. EDS verified the presence of Ca and Al as major constituents of the E-glass fibers (Fig. 6B). This EDS information can be contrasted with the EDS spectrum from material from the planar region of fracture (Fig. 7A). Fibers in this region failed at low stresses (~689 MPa)). EDS of these fibers (Fig. 7B) indicated Ca and Al depletion.

The design of the acid vessel incorporates a top cover, provide support for pipes and valves. During routine valve maintenance sulfuric acid was spilled onto the top of the vessel and subsequently rinsed off with water. The fit of the top cover on the vessel provided a mechanism to trap acid and/or acid rinse water in the vicinity of the circ wrap. Given this opportunity for

exposure of the fibers to sulfuric acid, it is quite probable that Ca and Al were leached from the fibers by the acid.^{2,3} Acid dissolution of Ca and Al significantly reduces the tensile strength of E-glass fibers,² consistent with our fractographic measurements. Further analysis of deposits on the fracture surface indicated the presence of $\text{Ca}(\text{SO}_4)_2$, a likely product of prolonged exposure of the material to sulfuric acid.

The failed vessel was examined for cracks in regions other than the primary fracture surface using a simple optical inspection technique. A fiber optic light source is placed against the surface of the translucent FRP vessel. In this manner, light is internally scattered. With this vicinal illumination, cracks oriented normal to the surface scattered the light and were observable as shadows in the halo around the fiber optic light source as shown in Fig. 8. Magnification of 10-20X is helpful, but not necessary for detecting the cracks. Using this technique cracks were located in regions of the vessel away from the primary crack and in the companion unfailed vessel.

Circumferential cracks were found in the circ wraps of both vessels. The cracks were always located in the same axial region; within five cm of the upper "knuckle" transition from the dome top to the cylindrical wall of the vessel (see Fig. 1). This region is very close to, or may include the top of the gasketed upper cradle support band. The cracks varied in length from a fraction of a cm to more than 25 cm in length. There were indications that some cracks had joined with neighbors to form longer cracks. Several cracks intercepted the edge of a cut section and appeared to penetrate the circ wraps. None of these cracks penetrated the entire wall, so as to be visible on the interior surface. No hoop cracks were found on the interior of the vessel or at any other location on the exterior surface.

FINITE ELEMENT ANALYSIS

A finite element analysis of the pressure vessel was performed to estimate the stress state prior to failure. The stress estimates, along with experimentally determined material strengths, were essential factors in the determination of the vessel failure scenario. The pressure vessel was modeled as axisymmetric thereby neglecting any small asymmetries in the area of penetrations in the top of the vessel. 4308 four-noded quadrilateral elements, each with four integration points, were used in the model. To accurately resolve the stresses through the thickness of the vessel and in the failed region, the teflon layer was modeled with two elements through the thickness, the cross plies with three elements through the thickness, and the circ wrap was modeled with four elements through the thickness. Figures 9 and 10 show the model geometry and mesh. In modeling the orthotropic properties of the FRP, appropriate properties were assigned to both the (cross

plies) and (circ wrap). The teflon liner was modeled as an isotropic material. All materials were assumed to be linearly elastic. The cradle was modeled by radially constraining the model in the region of the cradle gasket. The applied loading was a net internal pressure of 0.31 MPa. The analysis was run on a CRAY YMP using the commercial finite element analysis code ABAQUS version 4.9.⁴

The analysis shows a region of high axial or longitudinal tensile stress (~49 MPa (7100 psi)) just above the cradle gasket in the region where cracks were observed. This high stress region is shown in Fig. 11. Such stresses would tend to cause cracking in the circ wrap if its strength is at or below this level.

MECHANICAL TESTING

Flexural strength tests (three-point bend) were conducted to obtain the strength of uncracked composite material in the region where elevated tensile stresses were predicted (just above the metal cradle). Flexural strength specimens were also made from cracked material (cracks located by vicinal inspection technique) in this region to compare the fracture surfaces. Specimens were 5.1 mm thick by 22.9 mm wide by 83.8 mm long. Specimens were cut from the vessel and loaded such that the circ wrap layers from the exterior of the vessel were in tension, with the glass reinforcement fibers oriented perpendicular (normal) to the applied stress. The span was 69.9 mm and specimens were loaded at 0.13 mm/min.

The initial failure mode was matrix cracking in the circ wrap. Under continued loading, the crack continued to propagate through the matrix of the circ wrap until it reached the circ wrap/cross ply interface. Here the crack either changed direction and produced delamination of the circ wrap/cross ply interface, or continued along a tortuous path through the cross plies, with extensive fiber pull-out. The average tensile stress to initiate matrix cracking in uncracked specimens was 55 ± 9 MPa (8000 \pm 1325 psi). This value falls within the reported range of strengths for this type of material (28-62 MPa). This measured range of strengths is also within the predicted stress level of 49 MPa (7100 psi). Thus the tensile stresses developed under normal operating conditions (0.31 MPa internal pressure), in the region of the circ wraps adjacent to the cradle, are likely to have produced matrix cracking. Such cracks would then provide access to corrosive acid that attacked the glass fibers, degrading their strength. During each pressurization cycle weakened glass fibers failed, producing a slowly growing crack, which provided further access to acid, and failure of additional fibers. When the crack reached critical proportions, it propagated catastrophically and produced vessel failure.

As mentioned in the section describing the flexure specimens used for EDS analysis of glass fibers, when specimens from cracked and uncracked regions of the vessel in the vicinity of the circ wrap were examined, two types of fracture surfaces were observed. In the previously uncracked specimen, the fracture surface of the cross ply region exhibited the expected non-planar fracture with extensive fiber debonding and pull-out (Fig. 3B). In the specimens exhibiting pre-cracks in the circ wrap, the fracture surface of the cross ply region exhibited planar fracture with no fiber pull-out adjacent to the circ wrap, but non-planar fracture with extensive fiber pull-out in the remainder of the cross ply (see Fig. 3A). The arrangement (sequence) of these two types of fracture surfaces was similar to that observed on the primary cracks of the failed vessel. The presence of planar fracture in the cross ply material clearly demonstrates the existence of regions of extensive crack growth in the cross plies under normal operating pressures. Thus other cracks existed that could have eventually caused failure; the actual failure was not a fluke or the result of a unique flaw, but rather was simply the first cracked region to reach critical dimensions.

The proposed failure scenario and supporting evidence are summarized as follows:

- There were two primary circumferential through-cracks just above the steel cradle.
- The primary cracks were oriented parallel to the circ wrap direction and the fibers in the circ wrap.
- The fracture surface of the primary crack was planar even in the cross plies, with no evidence of fiber debonding or pull-out.
- The orientation of mirror, mist, and hackle features on glass fiber fracture surfaces from the planar region of the failed cross plies indicated that cracks initiated at the outer surface of the vessel and propagated inward.
- Fractographic evidence revealed that the load-bearing fibers on planar fracture surfaces in the cross ply region failed at 1/4 to 1/2 of their nominal strength, suggesting the possibility that environmental attack and strength degradation had occurred.
- Maintenance was performed on the valves on the top of the vessel, which resulted in sulfuric acid being spilled and washed down onto the region of the circ wraps.
- Microanalysis data showed that the Ca and Al contents of the weak E-glass fibers in the planar crack growth area were significantly reduced from that of full strength fibers elsewhere. The depletion levels and resulting strength degradation were similar to those reported in the literature for fibers of similar E-glass compositions after controlled exposure to sulfuric acid.
- Fractographic evidence indicated that fibers which failed during the final overload event (away from the initial

planar cracks) and during subsequent laboratory tests failed at full strength.

- Finite element calculations were performed for the vessel pressurized to 0.31 MPa under two conditions: with and without a stiff cradle. The radial constraint provided by the cradle produced a bending moment which resulted in a tensile stress of approximately 48 MPa in the axial direction of the vessel, on the outer surface, just above the cradle. This stress was transverse to the glass fibers in the circ wrap. Without the constraint of the cradle, a stress of this magnitude does not develop.
- Tensile tests were conducted on undamaged material cut from a region of the failed vessel away from the primary cracks. That material had an average strength of 55 ± 9 MPa, confirming that cracks could form in the circ wrap at the tensile stress levels produced by the radial constraint of the stiff steel cradle.
- Cracking of the matrix material of the circ wrap at the predicted stress levels provided access of acid to the fibers in the cross plies. Subsequent cracking of the cross plies proceeded non-catastrophically as acid-weakened fibers failed sequentially at the crack tip during subsequent pressurization cycles.
- A sample taken from an area which contained circumferential cracks, but away from the primary fracture, was broken in a three-point bend test. The fracture surface revealed a crack that penetrated about half way through the load-bearing cross plies. The planar character of this partial crack was similar to that observed on the two flat areas of the primary cracks.
- One or more cracks growing through the cross plies above the cradle reached the critical size for catastrophic crack propagation, resulting in vessel failure at normal operating pressure.

SUMMARY

A failure investigation was conducted on a ruptured sulfuric acid vessel. Forensic reconstruction of the event, fractographic analysis of the failed vessel, computer modeling of stresses in the vessel walls, and mechanical testing of sections of the failed vessel provided information about the probable cause of failure. It was concluded that the failure occurred at normal operating conditions and was the result of a localized high tensile stress causing cracking of the matrix, leading to acid-exposure and weakening of load-bearing glass fibers in the FRP. Sequential failure of weakened fibers led to crack growth during pressurization cycles until one crack reached the critical dimensions for catastrophic failure. Ceramic fractographic techniques and vicinal illumination were key elements in reconstructing the failure scenario.

REFERENCES

1. J. J. Mecholsky, "Fracture Surface Analysis of Optical Fibers," Engineered Materials Handbook, Vol. 4, Ceramics and Glasses, ASM 663-668 (1991).
2. B. Das, B. D. Tucker, and J. C. Watson, "Acid Corrosion Analysis of Fibre Glass," J. Mater. Sci. 26 [24] 6606-12 (1991).
3. B. D. Caddock, K. E. Evans, and I. G. Masters, "Diffusion Behaviour of the Core-Sheath Structure in E-Glass Fibres Exposed to Aqueous HCl," J. Mater. Sci. 24 [11] 4100-4105 (1989).
4. ABAQUS Version 4.9, Hibbitt, Karlsson, and Sorensen, Inc.

ACKNOWLEDGMENTS

This work was performed at Sandia National Labs, supported by the U.S. Department of Energy Under Contract #DE-AC04-76DP00789(??) and as part of Cooperative Research and Development Agreement 01082 with SEMATECH. The authors acknowledge SEMATECH, Intel Corporation, and Fluoroware, Inc. for permission to publish and present the results of this investigation. The authors also thank the other Sandia participants in this investigation including Mark Davis, John Geiske, Richard Grant, Fred Greulich, Chuck Gwyn, Will Hareland, Paul Hlava, Alice Kilgo, Bonnie McKenzie, Joe Michael, Gordon Pike, Ken Schuler, and Mark Stavig.

KEYWORD LIST

(3-8)

Fractography, fiberglass, epoxy, failure analysis, case study, acid attack, finite element analysis, vicinal illumination

LIST OF FIGURES

Fig. 1A. The FRP vessel contained several large cracks from which the burst teflon liner bulged. The region indicated with dashed lines was cut from the vessel for fracture surface examination (Fig. 2).

Fig. 1B. The FRP vessel failure also severely damaged the cabinet and showered the room with debris. (not sure whether we have a photo of this)

Fig. 2. Following an in situ examination of the ruptured vessel, a three by twenty inch section (section in dashed lines in Fig. 1), containing the primary fractures, was cut from the vessel for detailed examination. Macroscopic examination of the primary fracture surfaces revealed two areas (Areas A and B) of planar circumferential (or hoop) fracture, normal to the longitudinal axis of the vessel, extending almost completely through the circ wrap and cross plies.

Fig. 3A. Schematic cross section of the planar fracture surface observed for the circ wrap and cross plies of Area A.

Fig. 3B. Schematic cross section of the expected fracture surface topography for the circ wrap and cross plies.

Fig. 4. Schematic (A) and SEM micrograph (B) of hackle showing direction of crack propagation (note arrows).

Fig. 5A. The fracture surface of a flexure specimen which did not contain a pre-existing crack. There is no planar fracture in the cross ply regions (Area 2).

Fig. 5B. The fracture surface of a flexure specimen which contained a pre-existing crack in the circ wrap. The direction of crack propagation is from the bottom of the figure to the top. The photo shows the two types of macroscopic fracture features in the cross plies, i.e., the pre-existing crack exhibits planar fracture (Area 1), whereas the fracture surface produced during testing exhibits the expected fiber pull-out (Area 2).

Fig. 6A. SEM micrograph of a fractured fiber from a region of fracture exhibiting extensive fiber pull-out.

Fig. 6B. EDS verified the presence of Ca and Al as major constituents of E-glass fibers in the region of Fig. 6A.

Fig. 7A. SEM micrograph of a fractured fiber from a region of fracture exhibiting planar fracture (Fig. 5B, Area 1).

Fig. 7B. EDS of fiber from planar fracture region indicated depletion of Ca and Al relative to the EDS spectrum in Fig. 6B.

Fig. 8. Under vicinal illumination, cracks oriented normal to the surface scatter the light and are observable as shadows in the halo around the fiber optic light source (see arrows).

Fig. 9 Finite element model geometry and mesh of the FRP vessel and teflon liner.

Fig. 10 Detail of the finite element mesh of FRP vessel and teflon liner.

Fig. 11 Finite element analysis model showing stresses in FRP vessel wall. Regions of high tensile stress (~49 MPa) were found above the radial constraint of the cradle, and correspond to the cracked regions of the vessel.

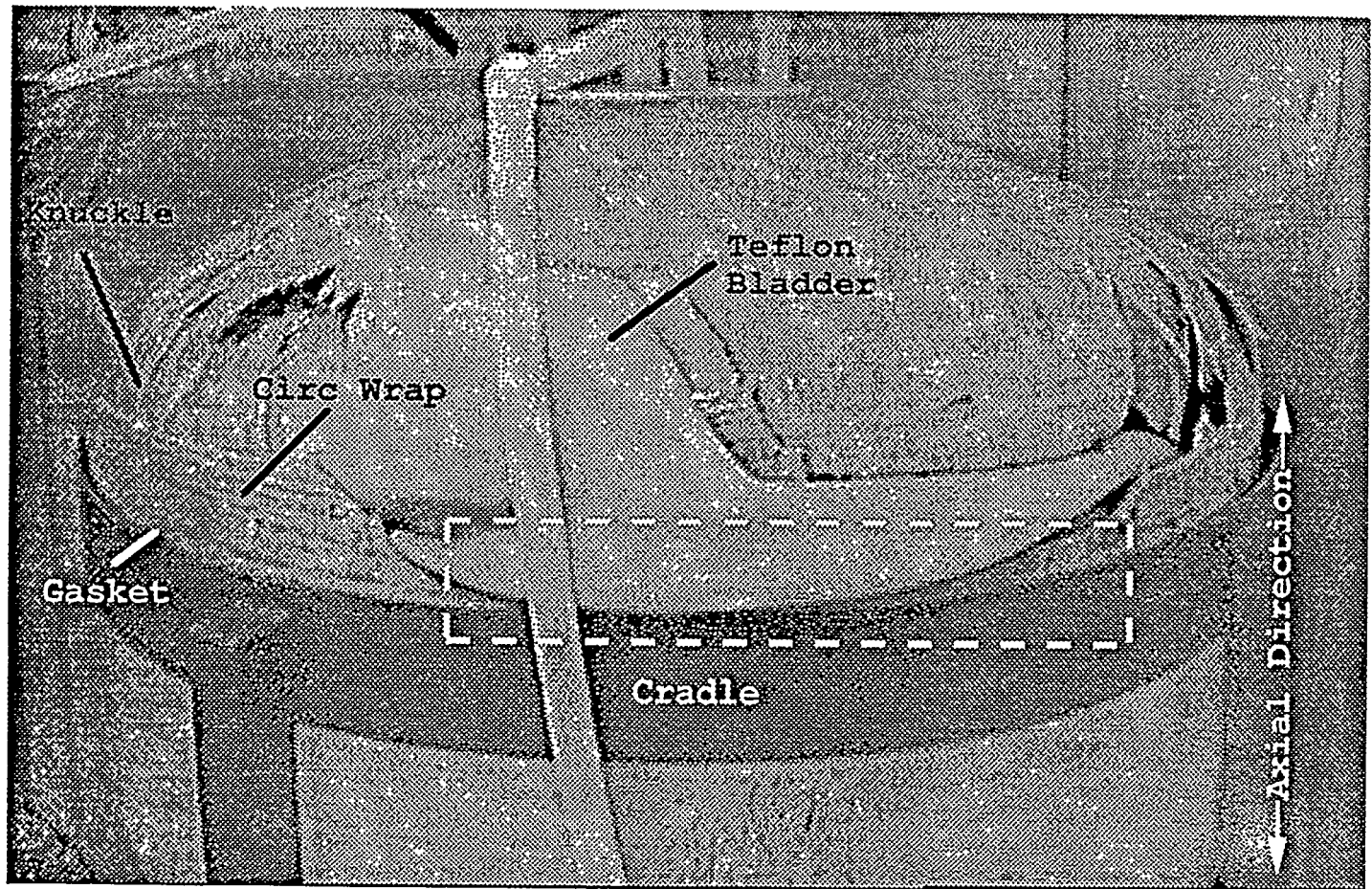
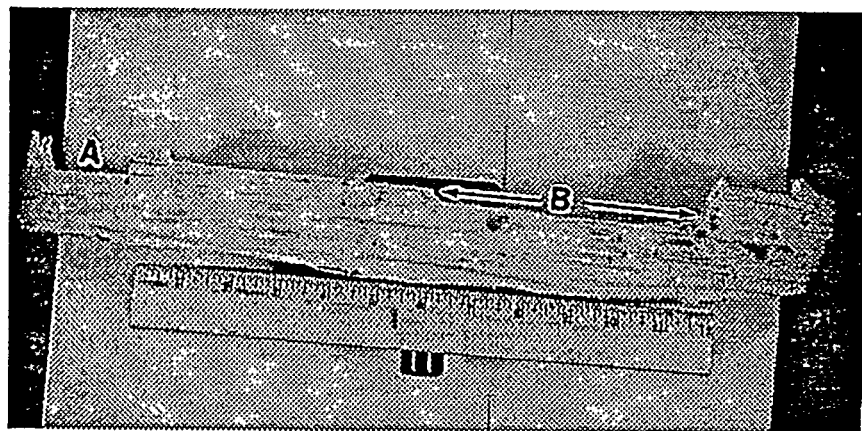
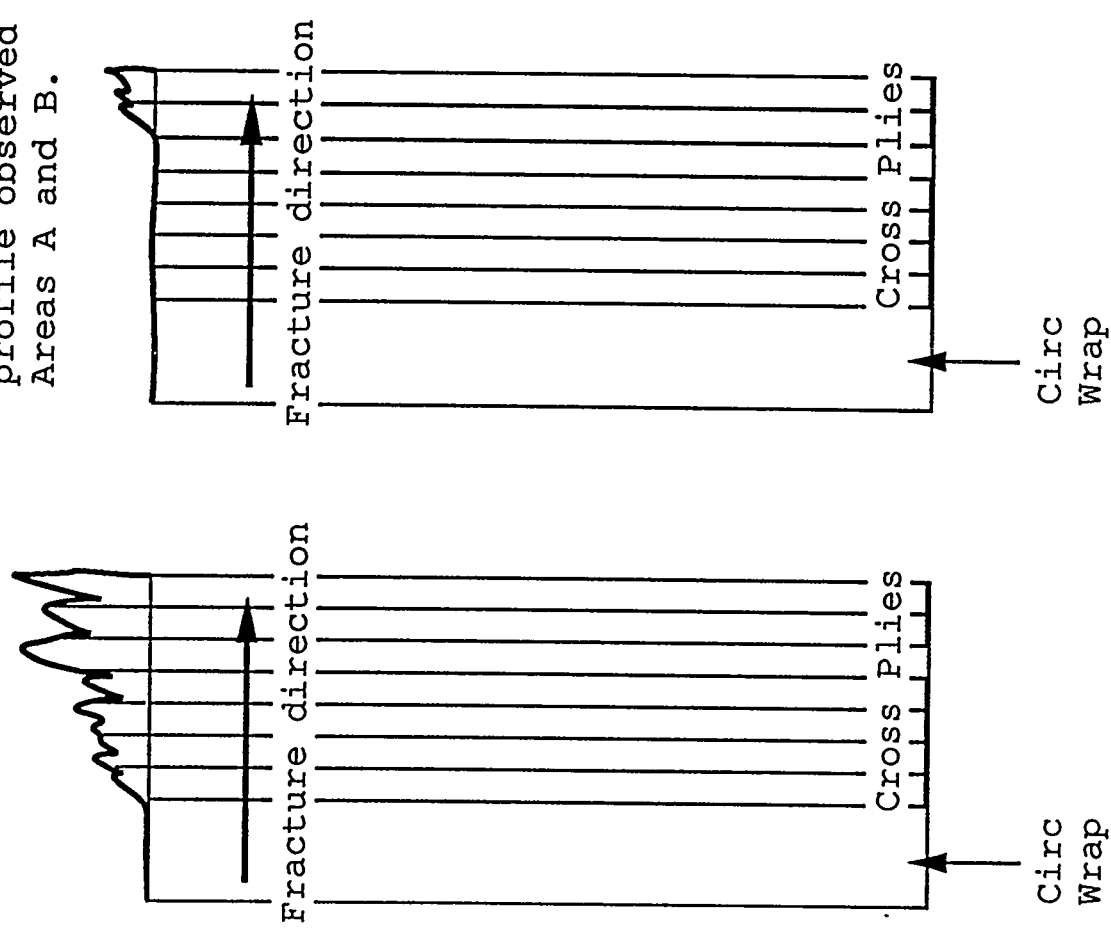




Fig. 1b

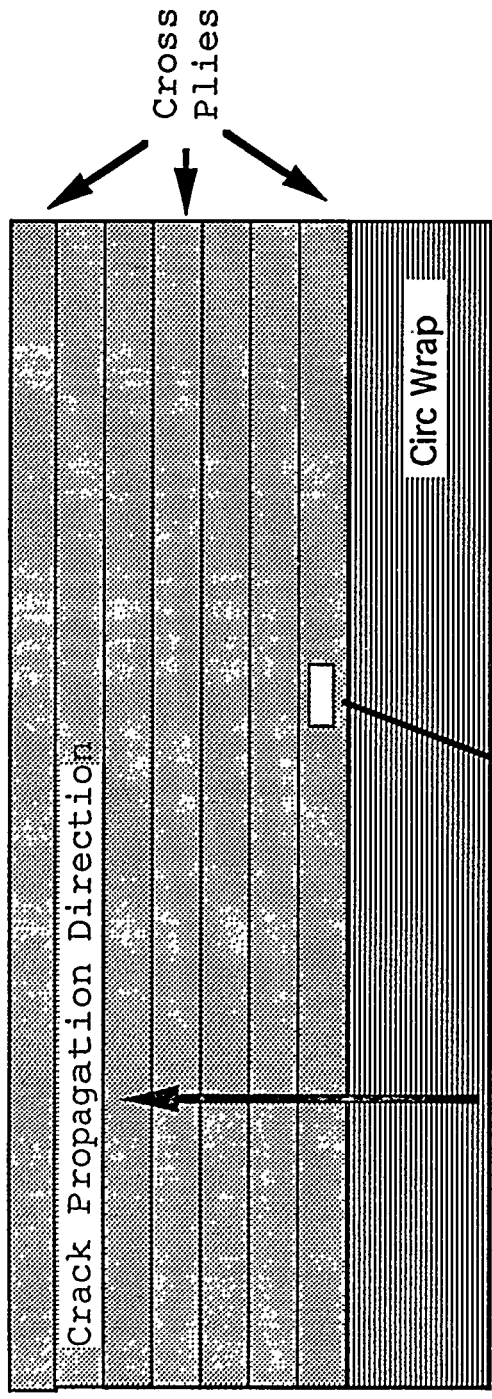


Normal fracture profile. Planar fracture profile observed in Areas A and B.

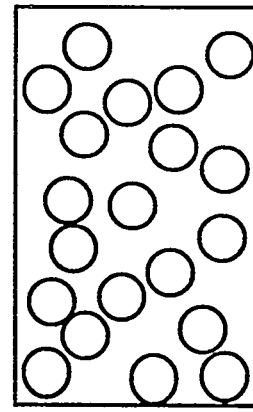


Fracture

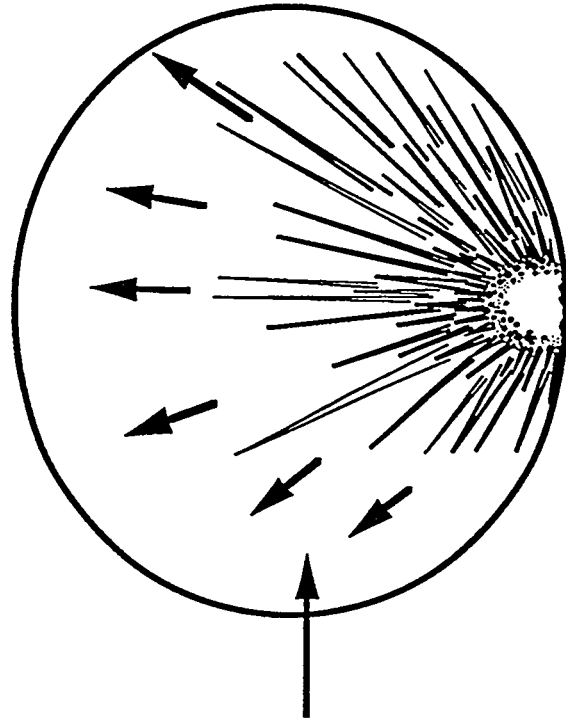
Vessel Interior



Vessel Exterior



Blow-up of cross
ply region.



Blow-up of individual
glass fiber. Hackle
marks indicate crack
propagation direction.



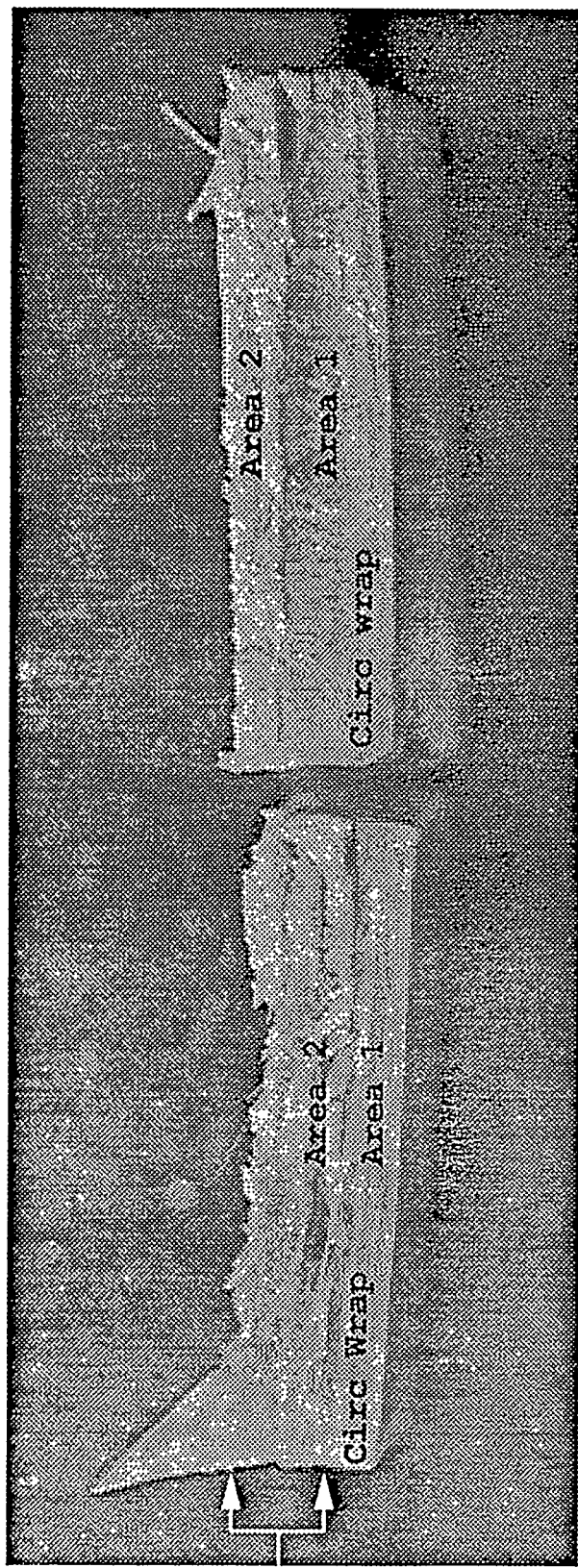
41-92-FRAC B AREA Z

x2000 10KV SNL

10μm

#0006

500



Cross
PLY
Region

Area 2

Area 1

Circ Wrap

Area 2

Area 1

Circ Wrap

B.

A.

Fig. 5

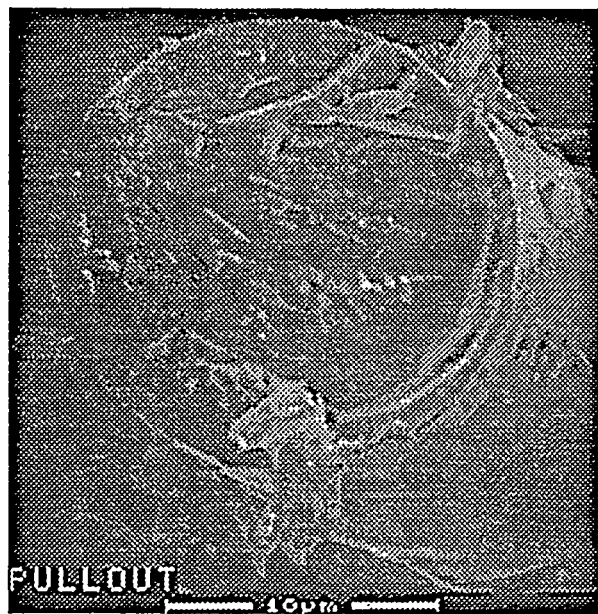
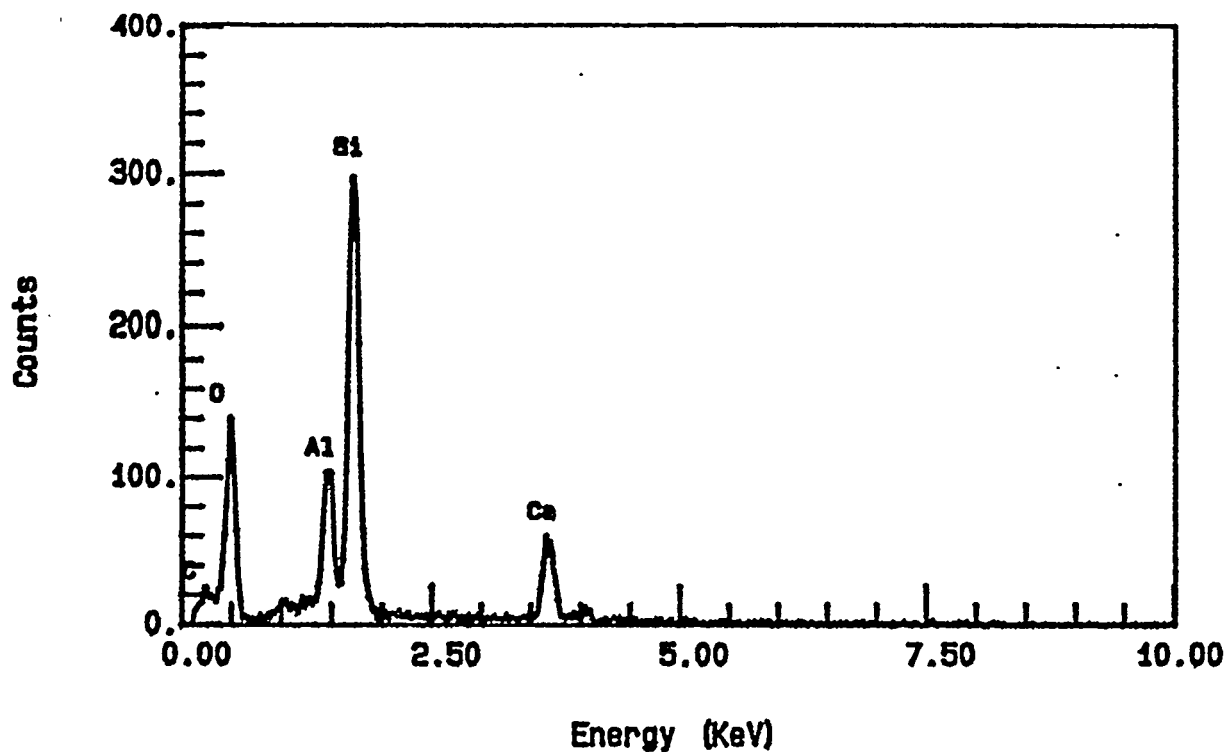


Fig. 6



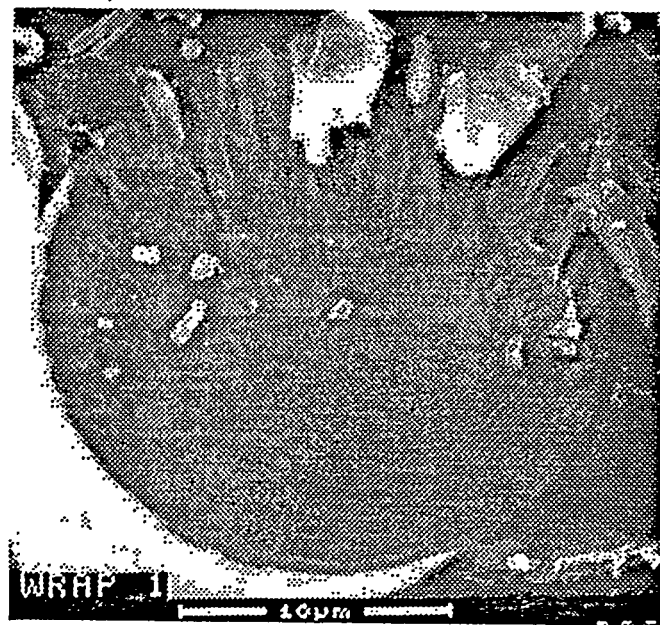


Fig. 1a

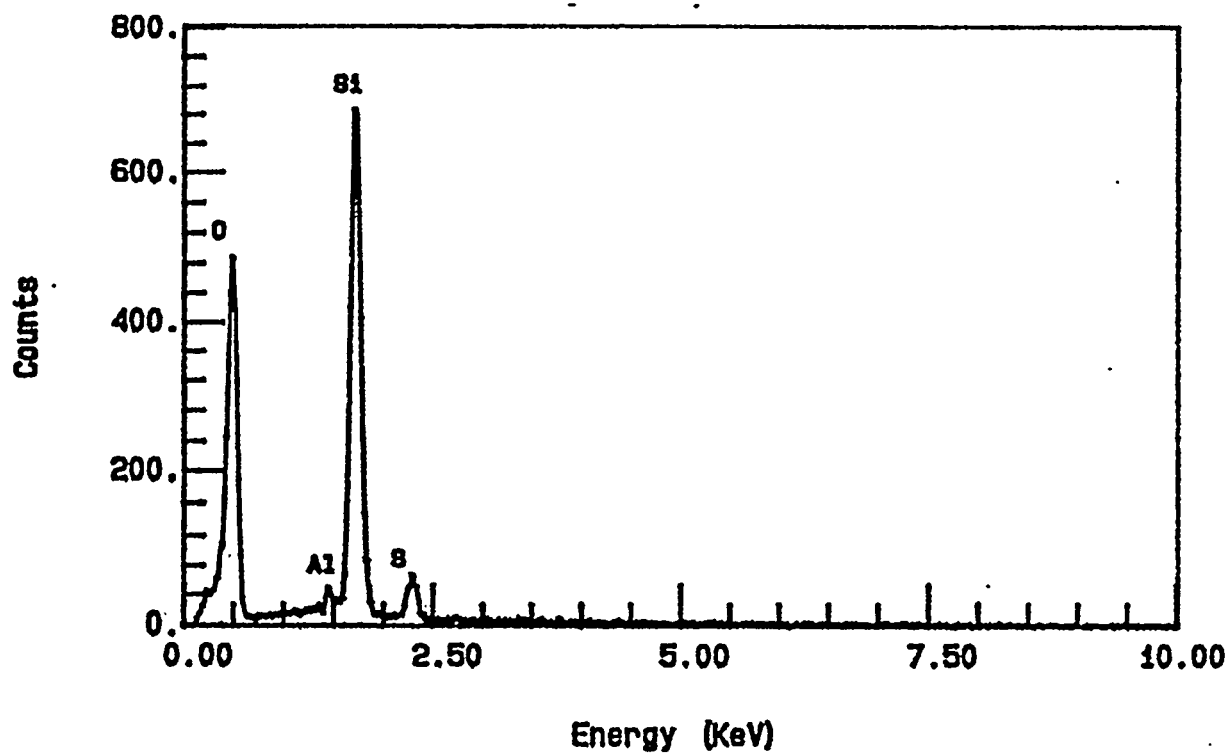
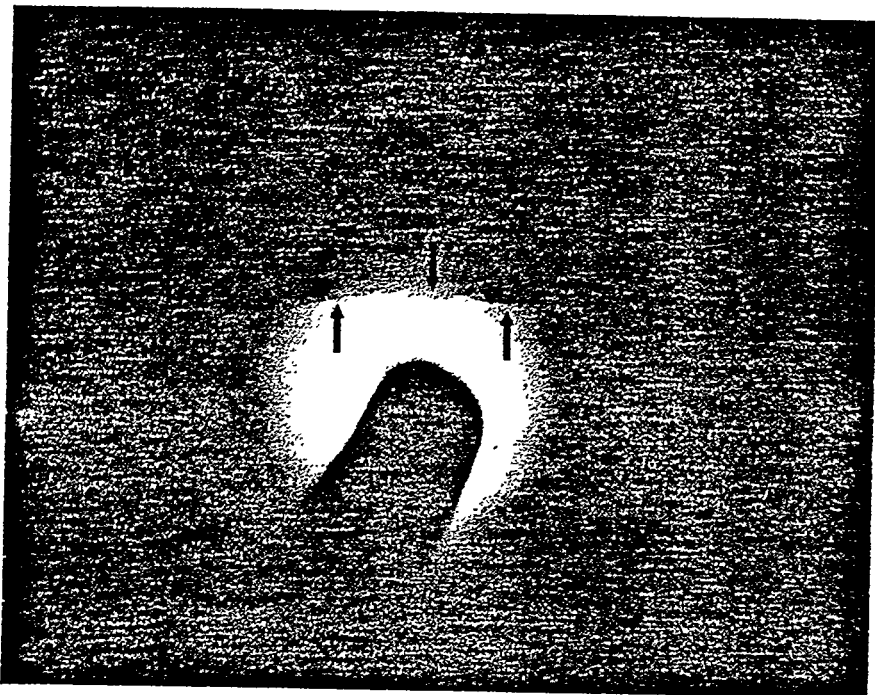


Fig. 2 b



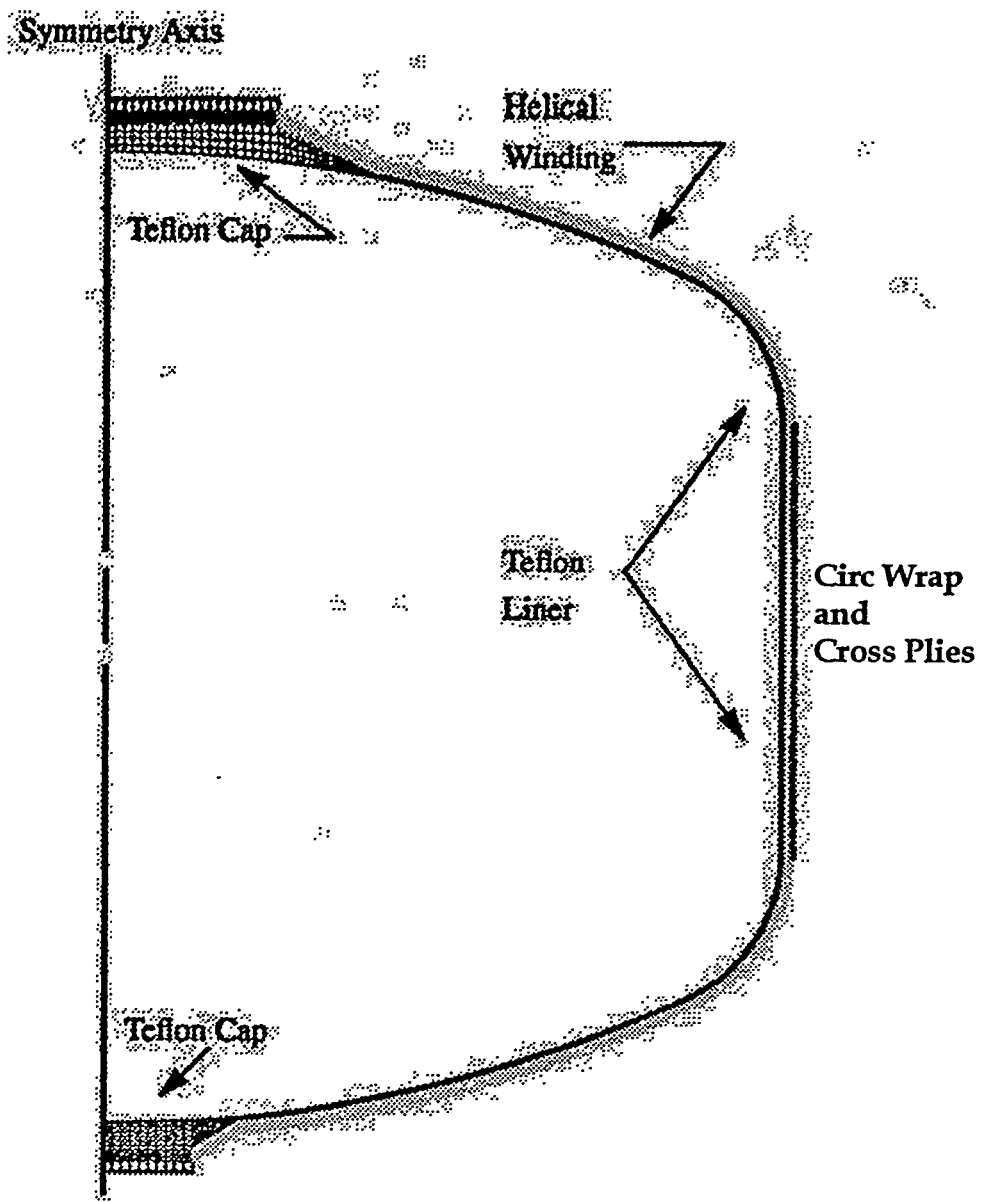
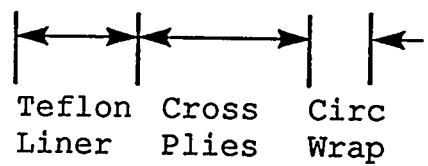
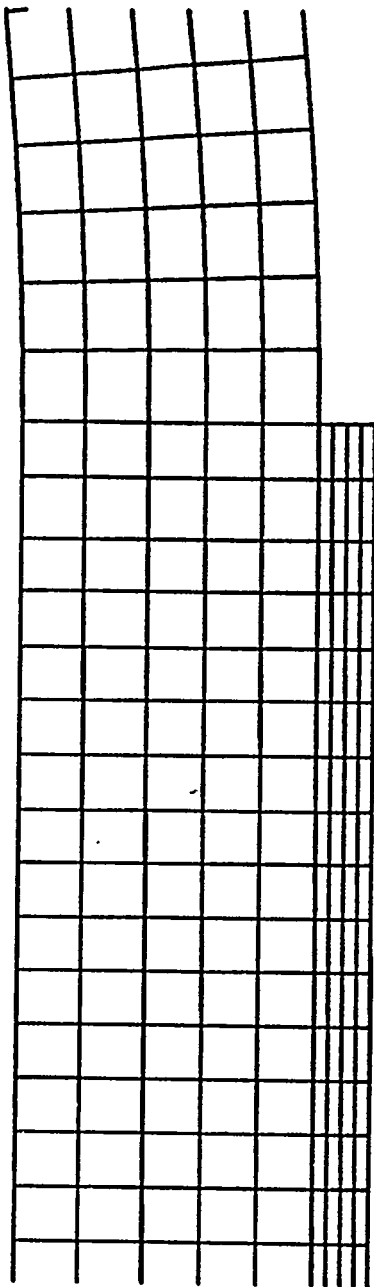
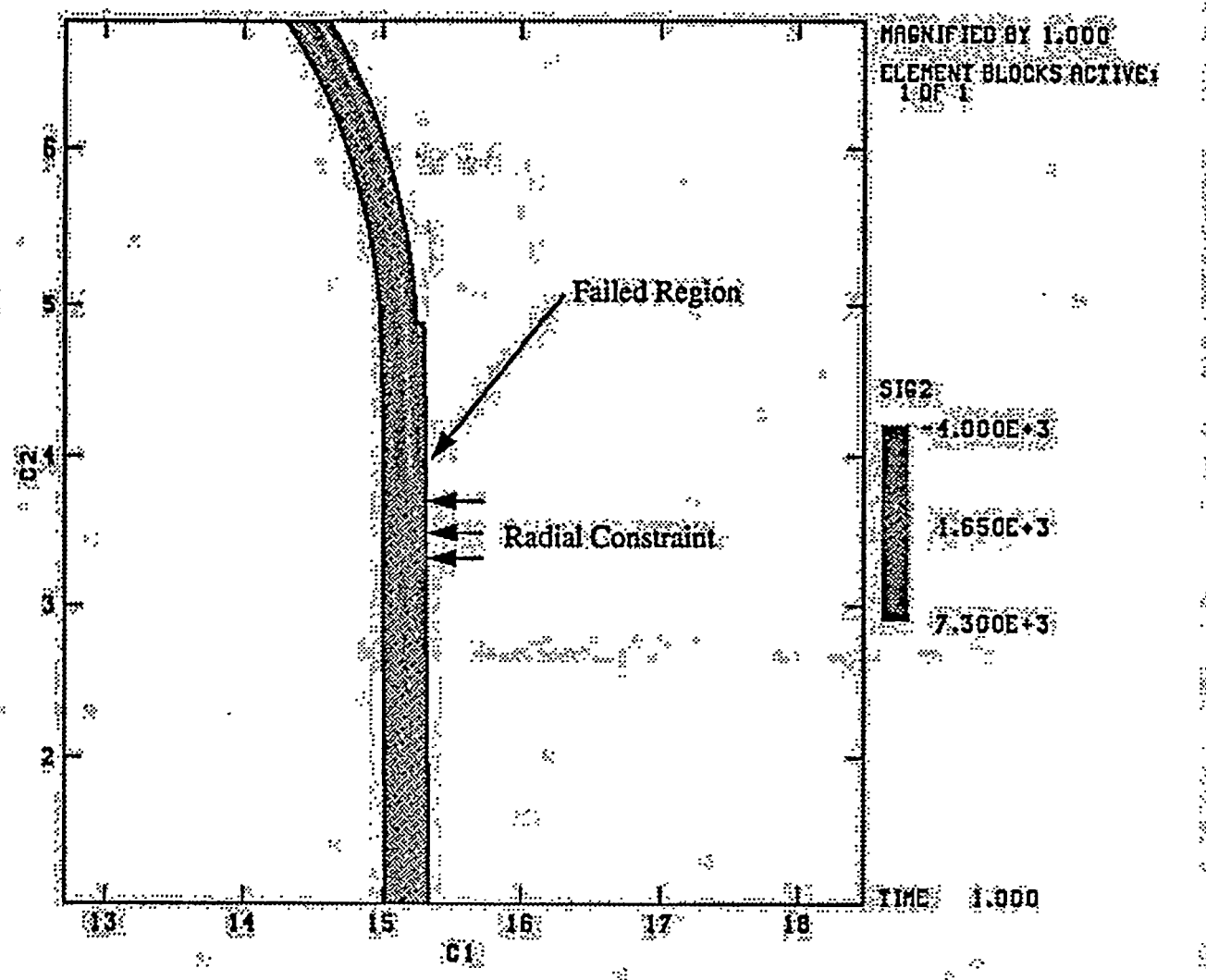


Figure 1. Finite Element Model Geometry and Mesh





DISCLAIMER

This report was prepared as an account of work sponsored by an agency of the United States Government. Neither the United States Government nor any agency thereof, nor any of their employees, makes any warranty, express or implied, or assumes any legal liability or responsibility for the accuracy, completeness, or usefulness of any information, apparatus, product, or process disclosed, or represents that its use would not infringe privately owned rights. Reference herein to any specific commercial product, process, or service by trade name, trademark, manufacturer, or otherwise does not necessarily constitute or imply its endorsement, recommendation, or favoring by the United States Government or any agency thereof. The views and opinions of authors expressed herein do not necessarily state or reflect those of the United States Government or any agency thereof.